NASA Technical Memorandum 81160

NASA-TM-81160 19800007776

A Comparison of Calculated and Experimental Lift and Pressure Distributions for Several Helicopter Rotor Sections

John Conlon

January 1980

National Aeronautics and
Space Administration

NASA Technical Memorandum 81160

A Comparison of Calculated and Experimental Lift and Pressure Distributions for Several Helicopter Rotor Sections

John Conlon, Ames Research Center, Moffett Field, California

NASA
National Aeronautics and
Space Administration

Ames Research Center
Moffett Field, California 94035

A COMPARISON OF CALCULATED AND EXPERIMENTAL LIFT AND PRESSURE DISTRIBUTIONS FOR SEVERAL HELICOPTER ROTOR SECTIONS

John Conlon

Ames Research Center

SUMMARY

The use of computational techniques in predicting lift coefficients and pressure distributions of two-dimensional airfoil sections was studied. The computer code FL06/IBL was used to solve the compressible, two-dimensional flow about four different airfoil sections. The lift coefficients of the airfoils were calculated at various angles of attack at subsonic Mach numbers. These calculated lift coefficients were then compared with experimental data. Good agreement between the experimental and calculated data in both lift-curve slope and values of lift coefficient was obtained. For three of the airfoils, calculated pressure distributions were also compared with experimental results for selected cases of Mach numbers and angles of attack; agreement between the calculated and experimental values was excellent.

INTRODUCTION

It is very desirable to be able to compare the aerodynamic characteristics of different helicopter rotor sections. Experimental airfoil aerodynamic data are not always readily available, however, and the data that are available usually have been obtained in different wind tunnels. This makes the comparison of the data difficult and uncertain because of differences in tunnel characteristics and in methods of correcting for the influence of the tunnel wall effects. Therefore, it is worthwhile to develop a unified method with which the airfoil section data can be compared on a uniform basis. One such approach is to use a computational technique that matches the data well.

In this study a computer code designed to solve the compressible flow about two-dimensional airfoil sections, FL06/IBL, was used to calculate the aerodynamic characteristics of several helicopter airfoil sections. The sections were the Boeing VR-7, Wortman 69-H-098, NACA 0012, and Ames-1 airfoils. The lift coefficients and pressure distributions of these airfoils were calculated at angles of attack from 0° to 12° and at Mach numbers of 0.3 to 0.6; the results were then compared with wind-tunnel test data.

METHOD OF SOLUTION

The FL06/IBL computer code consists of two separate programs: the main program, FL06 (ref. 1), solves the potential flow about the airfoil; the second program, IBL (refs. 2 and 3), solves for the boundary layer on the airfoil. By coupling these two programs and performing a number of iterations to account for the boundary-layer displacement thickness, a solution for the viscous flow about the airflow is obtained.

FL06 is a two-dimensional, inviscid, compressible-flow code. It uses conformal mapping, or mapping from an airfoil to a circle, to solve the potential flow about the airfoil. The program first calculates the local velocities and pressure coefficients over the airfoil and then integrates the pressure coefficients over the surface of the airfoil to produce lift and drag coefficients. Since FL06 is inviscid, however, the drag coefficient calculated by the program is zero. The pitching moment coefficient is calculated about the quarter-chord, using the calculated lift and drag pressure coefficients.

IBL uses the pressure distribution from FL06 to solve the two-dimensional boundary-layer equations. The displacement thickness, momentum thickness, and the local coefficient of friction are determined. The coefficient of friction is then used to determine the point of flow separation; the criterion of flow separation is a negative friction coefficient. The boundary-layer displacement thickness calculated in IBL is added to the original airfoil surface, giving a new airfoil configuration. The potential flow about this airfoil is solved and its lift coefficient is compared with the lift coefficient calculated previously. The solution is assumed to be converged when the lift coefficient varies by less than 2% in two successive computations.

CONFIGURATIONS AND CONDITIONS

Four airfoils were studied: the Boeing VR-7, the Wortman 69-H-098, the NACA 0012, and the Ames 1. The airfoils are shown in figure 1 and their coordinates are listed in tables 1-4. These airfoils were chosen because wind-tunnel test data are available for them.

The experimental results for the Boeing VR-7 airfoil were taken from reference 4, which reported the results of tests conducted in the 1- by 3-ft subsonic insert of the Boeing Supersonic Wind Tunnel at Seattle, Washington. The experimental results from tests conducted in the 2.75- by 7.75-ft insert of United Aircraft Research Laboratories' 8-Foot Subsonic Wind Tunnel were used for the Wortman 69-H-098 airfoil (ref. 5). The experimental data from reference 6 were used for the NACA 0012 airfoil; reference 6 did not mention what wind tunnel was used to test the airfoil. For the Ames-1 airfoil, the experimental data were obtained from reference 7, which reports the results of wind-tunnel tests conducted in the Ames 2- by 2-Foot Transonic Wind Tunnel.

The thickness-to-chord ratios of the four airfoils are as follows: (1) the Boeing VR-7 and NACA 0012 — 12%; (2) the Wortman 69-H-098 — 9.8%, and (3) the Ames-1 — 10%. The Boeing VR-7 airfoil also has a trailing edge tab of 3° deflection.

The lift coefficients and pressure distributions were calculated for angles of attack from 0° to 12° and for Mach numbers of 0.3 to 0.6. The Reynolds numbers for the calculated results were based on unit chord and varied only with speed. The Reynolds numbers were chosen to approximate standard sea level conditions.

RESULTS AND DISCUSSION

Coefficient of Lift

Plots of coefficient of lift vs angle of attack at several different Mach numbers for each airfoil are presented in figures 2 to 15. Note that even though the experimental and theoretical Reynolds numbers were not the same in most cases, the differences are not expected to have a significant effect.

The lift coefficients for the Boeing VR-7 airfoil are shown in figures 2 to 5. Lift coefficients were calculated at several different angles of attack for Mach numbers of 0.3, 0.4, 0.5, and 0.6. Excellent agreement is shown between calculated and experimental results, both in lift-curve slope and in the magnitude of the lift coefficient; the results agree up to the higher angles of attack, where boundary-layer separation effects become dominant. The disagreement at the higher angles of attack is believed to be due to a poor model for computing the flow, once boundary-layer separation occurs. In the flow model reported here, the viscous, separated layer is approximated by a straight-line extrapolation of the boundary-layer displacement thickness, as calculated by IBL at the two upstream points preceding separation. However, experimental results show that the change in the displacement thickness during separation more closely resembles a parabolic curve than a straight line (ref. 8). Nevertheless, a straight-line extrapolation was used for convenience.

The results for the Wortman 69-H-098 airfoil are shown in figures 6 to 8. Plots for coefficients of lift are shown for Mach numbers of 0.30 (fig. 6), 0.50 (fig. 7), and 0.60 (fig. 8). The calculated results agree very closely with experimental data, especially for the slopes of the lift coefficient curves. Values of lift coefficient were not calculated for the Wortman 69-H-098 airfoil at Mach numbers of 0.50 and 0.60 (nor for the Boeing airfoil at $M = 0.60$) at the higher angles of attack; at those Mach numbers, the local flows on these airfoils become supersonic and shock waves form. The shock waves, in turn, produce discontinuous pressure rises of sufficient magnitude to cause the IBL code to predict boundary-layer separation. No approximate flow model has been developed for the case of shock-induced separation and therefore no force coefficients are given beyond the angles of attack where

that separation occurs. Although the flow would separate due to the shock wave, it would also most likely reattach downstream. This is seen in the experimental data which show that the lift continues to increase to much higher angles of attack than those predicted by the calculation.

The lift coefficients for the NACA 0012 airfoil were calculated for Mach numbers of 0.3, 0.4, 0.5, and 0.6. The calculated results and experimental results are shown in figures 9 to 12. The calculated lift coefficients agree very closely with the experimental values up to flow separation. However, the slope of the lift curve for the calculated results is slightly higher than the lift-curve slope of the experimental results.

The lift coefficients for the Ames-1 airfoil at Mach numbers of 0.30, 0.40, and 0.60 are shown in figures 13 to 15. The lift-curve slopes for the calculated lift coefficients agree closely with the experimental results. Except for the 0.20 Mach number case, however, the calculated lift coefficients do not match those predicted from experiment; the calculated values are lower than the experimental values at $M = 0.40$ and 0.60. This is most likely due to an insufficient correction of the experimental results for wind-tunnel wall effects.

For the four airfoils presented, the differences between the experimental and calculated results have been attributed to two sources. The first is inaccuracies within the computational model, such as the method by which the program handles flow separation, as discussed previously. There is also a possible 2% difference in the calculated lift coefficients because of the convergence criteria within the program. The other source of error is the influence on experimental results of the wind-tunnel wall correction method that was used. The wall corrections result in an incremental change in angle of attack, which increases with increasing Mach number and with increasing absolute value of angle of attack. Therefore, the data from similar airfoils tested in different wind tunnels can very often be different. This is true of all the wind tunnels although it is more apparent in the results from the Ames 2- by 2-Foot Wind-Tunnel test.

It is these differences between wind tunnels and between wall correction methods used that makes comparisons of data obtained from different tunnels uncertain and inaccurate. However, in the design and analysis of airfoils it is often worthwhile to compare the aerodynamic characteristics of different airfoils. This creates the need for a single method that would enable valid comparisons to be made. The computer code studied here, FL06/IBL could be used for such a purpose. It closely predicts the lift characteristics and could be used to make relative comparisons of the aerodynamic characteristics of different airfoils.

Pressure Profiles

The calculated pressure distributions of the Wortman 69-H-098, NACA 0012, and the Ames-1 airfoils were also compared with experimental data; the variations of pressure coefficients with chords are shown in figures 16 to 22. The experimental data for the Wortman 69-H-098 airfoil and the NACA 0012

airfoil were obtained from reference 9, which reported results of tests conducted in the 6- by 28-in. transonic wind tunnel at Langley Research Center; the experimental data for the Ames-1 airfoil are from reference 7.

Shown in figures 16 and 17 are the pressure profiles for the Wortman airfoil at angles of attack of 0° and at 3° at a Mach number of 0.50. The agreement between the experimental pressure coefficients and the calculated values is excellent. The peak pressure and its calculated location closely match those prescribed by experiment.

Figure 18 shows the pressure profiles for the NACA 0012 airfoil at $M = 0.50$ and at an angle of attack of 0°; the profiles at $M = 0.50$ at an angle of attack of 3° are shown in figure 19. At 0° angle of attack, the calculated pressure profile matches the experimental results very well and (as is to be expected for symmetrical airfoils) shows identical pressure coefficients for the upper and lower surface. The calculated pressure coefficients for the 3° angle-of-attack case also agree very closely with the experimental data.

Figures 20 to 22 show the pressure profiles for the Ames-1 airfoil. Plots of the pressure coefficients are shown for Mach numbers of 0.20 (fig. 20), 0.40 (fig. 21), and 0.60 (fig. 22); all are shown at angles of attack of 2°. The calculated pressure distributions match those obtained from experiment, but not as well as data for the Wortman and NACA airfoils. The experimental pressure profiles show slightly lower peak pressure coefficients than were calculated, and slightly higher pressure coefficients near the trailing edge. The differences between experimental and calculated peak pressure coefficients increase with increasing Mach number. However, these differences in pressure coefficients could possibly be due to an insufficient correction being applied to the data for wind-tunnel wall effects. Wall effects would cause the corrected angle of attack to be lower than the geometric angle of attack and, therefore, the pressure coefficients could be too low by a slight amount. The angles of attack of the Wortman 69-H-098 airfoil and the NACA 0012 airfoil were corrected for wall effects.

CONCLUSIONS

The calculated lift coefficients of the Boeing VR-7 and the Wortman 69-H-098 airfoils agreed very well with the experimental results, both in lift-curve slope and in the magnitude of the lift coefficients. However, the lift coefficients calculated for the Ames-1 airfoil were less than the experimentally-determined coefficients; the calculated results for the NACA 0012 airfoil were slightly higher than the experimental results.

The calculated pressure profiles of the Wortman 69-H-098 and the NACA 0012 airfoils showed excellent agreement with experimental results. The pressure coefficients of the Ames-1 airfoil also agreed very well with the experimental data, except that the calculated pressure peaks were slightly higher than the experimental ones.

Overall, the coefficients of lift and pressure calculated by FL06/IBL computer code compared well with experimentally-determined coefficients. The theoretical and experimental results compare well only when wall effects are accounted for and only for a restricted class of flows, that is, no separation. Improvements in the following areas, however, would greatly increase the usefulness of the computer code:

1. A drag prediction subroutine should be added.

2. The computer code should be modified so that the boundary layer reattaches after the separation caused by the formation of a shock wave on the airfoil.

3. The model of the separated flow on the airfoil should be changed from a straight-line extrapolation to one that would correspond more closely to the real flow.

REFERENCES

1. Jameson, A.: Iterative Solution of Transonic Flows Over Airfoils and Wings Including Flows at Mach 1. Commun. Pure Appl. Math., vol. 27, 1974, pp. 283-309.

2. Murphy, J. D.; and Davis, C. B.: Users Guide — Ames Inlet Boundary Layer Program MK-1. NASA TMX-62,211, 1973.

3. Murphy, J. D.; Presley, L. L.; and Rose, W. C.: On the Calculation of Supersonic Separating and Reattaching Flows. Part I. Aerodynamic Analysis Requiring Advanced Computers, Ames Research Center, NASA, Mar. 1975, pp. 151-175.

4. Dadone, L. U.: U.S. Army Helicopter Design Datcom. Vol. 1, Airfoils. Boeing Company, Boeing Doc. No. D210-11097-1, May 1976.

5. Shephard, W.; and Griffin, T.: Wind Tunnel Tests of Bell Two-Dimensional Aircraft Models. United Aircraft Research Laboratories, Report No. J930980-1, May 1970.

6. Kemp, L. D.: An Analytical Study for the Design of Advanced Rotor Airfoils. NASA CR-112297, 1973.

7. Hicks, R.; and McCrosky, W. J.: An Experimental Evaluation of a Helicopter Rotor Section Designed by Numerical Optimization. NASA TM-78622, 1979.

8. Seetharam, H. C.; and Wventz, W. H.: Experimental Studies of Flow Separation and Stalling on a Two-Dimensional Airfoil at Low Speeds. NASA CR-2560, 1975.

9. Noonan, K. W.; and Bingham, B. V.: Two-Dimensional Aerodynamic Characteristics of Several Rotorcraft Airfoils at Mach Numbers from 0.35 to 0.90. NASA TMX-73990, 1977.

TABLE 1.- COORDINATES:
BOEING VR-7 AIRFOIL

x	y	
	Upper surface	Lower surface
0.000000	0.000000	0.000000
.000200	.002104	-.002082
.000500	.003366	-.003304
.001000	.004828	-.004604
.002000	.006961	-.006331
.003500	.009428	-.008000
.005000	.011488	-.009189
.006500	.013298	-.010100
.008000	.014942	-.010857
.010000	.016950	-.011720
.012500	.019232	-.012626
.016000	.022129	-.013673
.020000	.025119	-.014672
.025000	.028459	-.015748
.035000	.034229	-.017508
.050000	.041444	-.019658
.065000	.047593	-.021540
.080000	.052994	-.023203
.100000	.059215	-.025159
.125000	.065651	-.027092
.150000	.070906	-.028549
.200000	.078870	-.030547
.250000	.083783	-.031863
.300000	.085924	-.032726
.350000	.085742	-.033085
.400000	.083650	-.032709
.450000	.079841	-.031480
.500000	.074514	-.029516
.550000	.067807	-.027124
.600000	.059965	-.024644
.650000	.051714	-.022074
.700000	.043219	-.019291
.750000	.034418	-.016390
.800000	.025274	-.013464
.850000	.015754	-.010498
.900000	.005578	-.007443
.925000	.001168	-.006089
.950000	-.000162	-.005120
.975000	.001149	-.003798
.990000	.001944	-.003003
1.000000	.002473	-.002473

TABLE 2.- COORDINATES:
WORTMAN 69-H-098 AIRFOIL

x	y	
	Upper surface	Lower surface
0.000000	0.000000	0.000000
.000500	.002929	-.002485
.001000	.004262	-.003430
.002000	.006190	-.004710
.003500	.008367	-.006087
.005000	.010171	-.007167
.006500	.011755	-.008071
.008000	.013193	-.008858
.010000	.014940	-.009782
.012500	.016925	-.010793
.016000	.019440	-.012017
.020000	.022045	-.013215
.025000	.025010	-.014508
.035000	.030210	-.016638
.050000	.036807	-.019131
.065000	.042342	-.021115
.080000	.047055	-.022773
.100000	.052219	-.024643
.125000	.057135	-.026579
.150000	.060730	-.028190
.200000	.064910	-.030591
.250000	.066499	-.031982
.300000	.066304	-.032508
.350000	.065154	-.032416
.400000	.063360	-.031845
.450000	.060968	-.030960
.500000	.057984	-.029819
.550000	.054448	-.028427
.600000	.050402	-.026779
.650000	.045857	-.024874
.700000	.040851	-.022730
.750000	.035427	-.020339
.800000	.029624	-.017682
.850000	.023365	-.014729
.900000	.016422	-.011335
.925000	.012529	-.009321
.950000	.008557	-.007018
.975000	.004759	-.004228
.990000	.002555	-.002367
1.000000	.001099	-.001099

TABLE 3.- COORDINATES:
NACA 0012 AIRFOIL

x	y	
	Upper surface	Lower surface
0.0000	0.0000	-0.0000
.0005	.0040	-.0040
.0010	.0056	-.0056
.0025	.0087	-.0087
.0050	.0122	-.0122
.0075	.0149	-.0149
.0100	.0170	-.0170
.0125	.0189	-.0189
.015	.0206	-.0206
.02	.0236	-.0236
.03	.0284	-.0284
.04	.0323	-.0323
.05	.0355	-.0355
.06	.0383	-.0383
.08	.0430	-.0430
.10	.0469	-.0469
.12	.0499	-.0499
.14	.0524	-.0524
.16	.0544	-.0544
.18	.0560	-.0560
.20	.0574	-.0574
.225	.0586	-.0586
.25	.0594	-.0594
.275	.0599	-.0599
.30	.0600	-.0600
.325	.0599	-.0599
.35	.0595	-.0595
.375	.0588	-.0588
.4	.0580	-.0580
.425	.0569	-.0569
.45	.0558	-.0558
.475	.0544	-.0544
.5	.0529	-.0529
.55	.0495	-.0495
.6	.0456	-.0456
.65	.0413	-.0413
.70	.0366	-.0366
.75	.0315	-.0315
.8	.0262	-.0262
.85	.0205	-.0205
.90	.0145	-.0145
.95	.0080	-.0080
1.00	.0013	-.0013

TABLE 4.- COORDINATES:
AMES-1 AIRFOIL

x	y	
	Upper surface	Lower surface
0.000000	0.000000	0.000000
.000200	.002379	-.002228
.000500	.003771	-.003375
.001000	.005414	-.004719
.002000	.007656	-.006512
.003500	.010133	-.008436
.005000	.012144	-.009945
.006500	.013878	-.011196
.008000	.015434	-.012270
.010000	.017315	-.013503
.012500	.019447	-.014815
.016000	.022136	-.016341
.020000	.024901	-.017770
.025000	.028006	-.019223
.035000	.033351	-.021367
.050000	.039906	-.023654
.065000	.045233	-.025486
.080000	.049610	-.027101
.100000	.054210	-.029016
.125000	.058287	-.031038
.150000	.060977	-.032767
.200000	.063435	-.035505
.250000	.064310	-.037272
.300000	.064461	-.038283
.350000	.064089	-.038655
.400000	.063156	-.038481
.450000	.061544	-.037820
.500000	.059237	-.036651
.550000	.056234	-.035013
.600000	.052486	-.032965
.650000	.047923	-.030558
.700000	.042460	-.027850
.750000	.036002	-.024857
.800000	.028604	-.021534
.850000	.020640	-.017857
.900000	.012596	-.013739
.925000	.008990	-.011435
.950000	.005979	-.008881
.975000	.003919	-.006027
.990000	.003216	-.004206
1.000000	.002994	-.003004

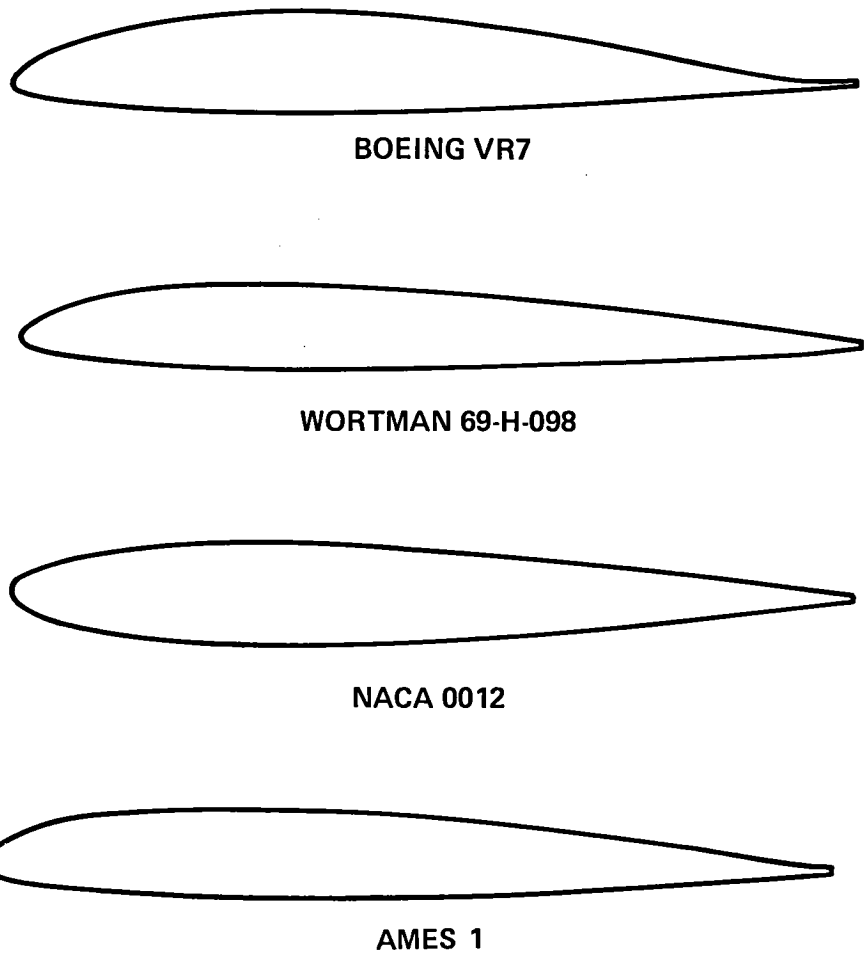

Figure 1.- Helicopter rotor sections.

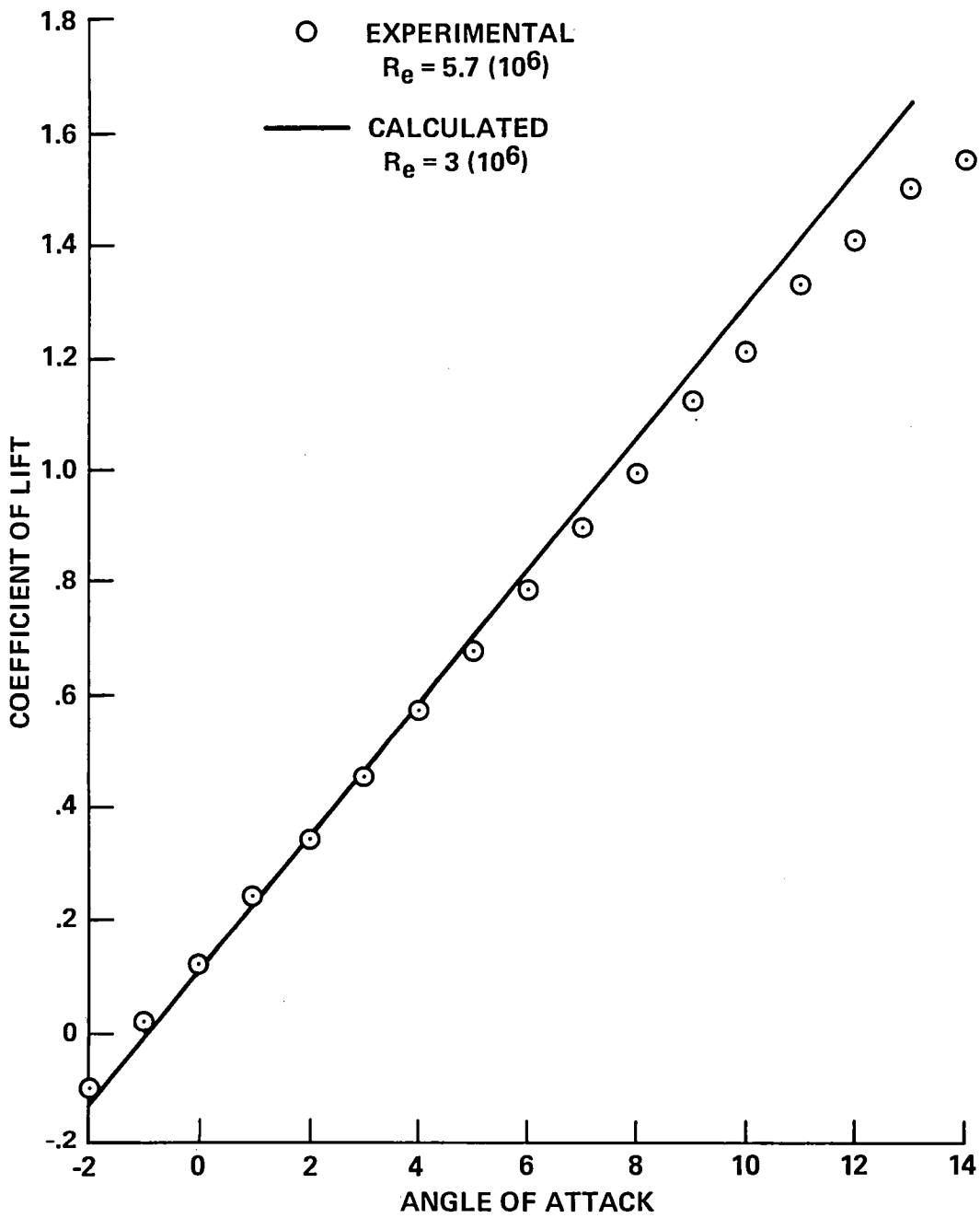

Figure 2.- Boeing VR-7 airfoil: coefficient of lift vs angle of attack at M = 0.3.

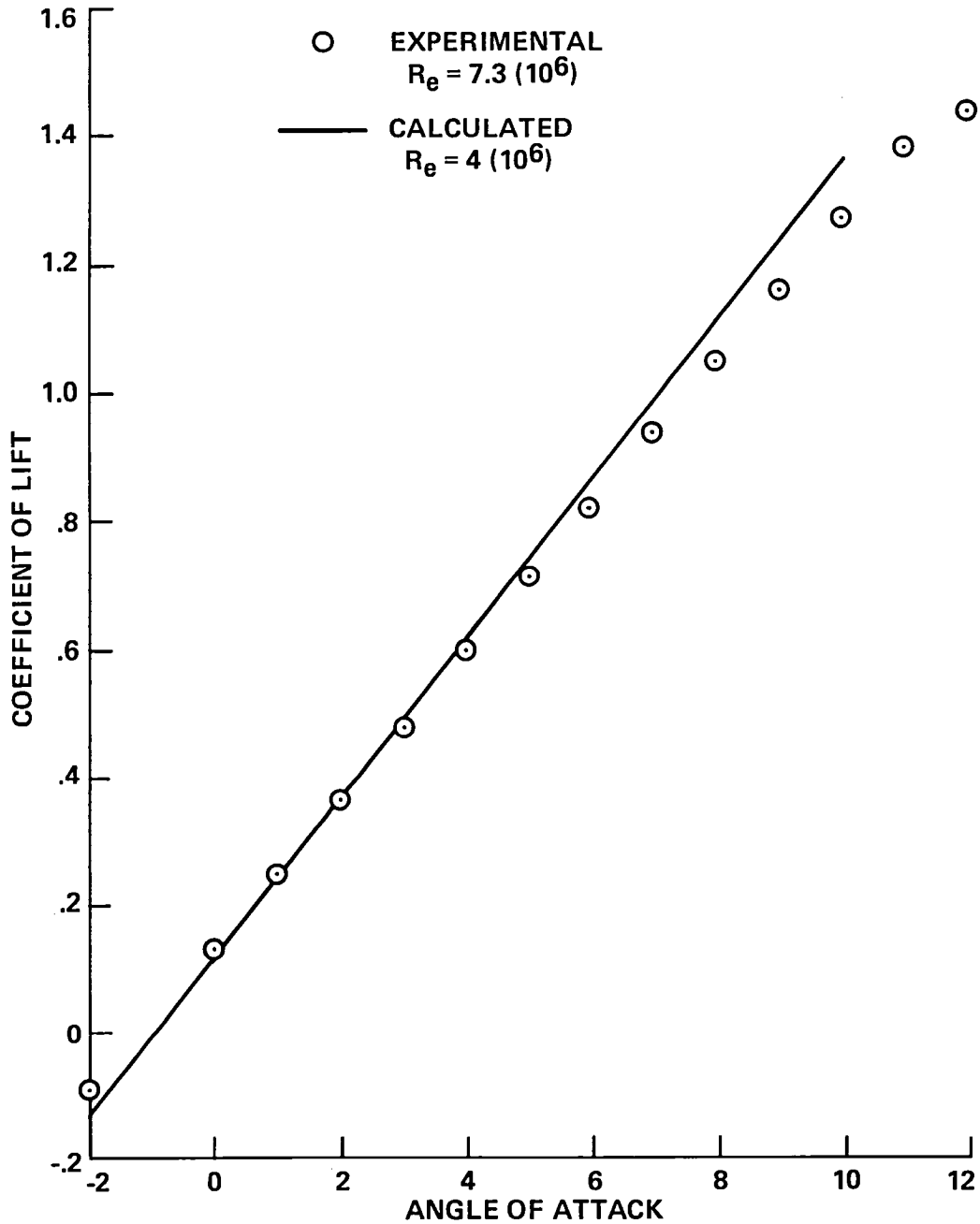

Figure 3.- Boeing VR-7 airfoil: coefficient of lift vs angle of attack at M = 0.4.

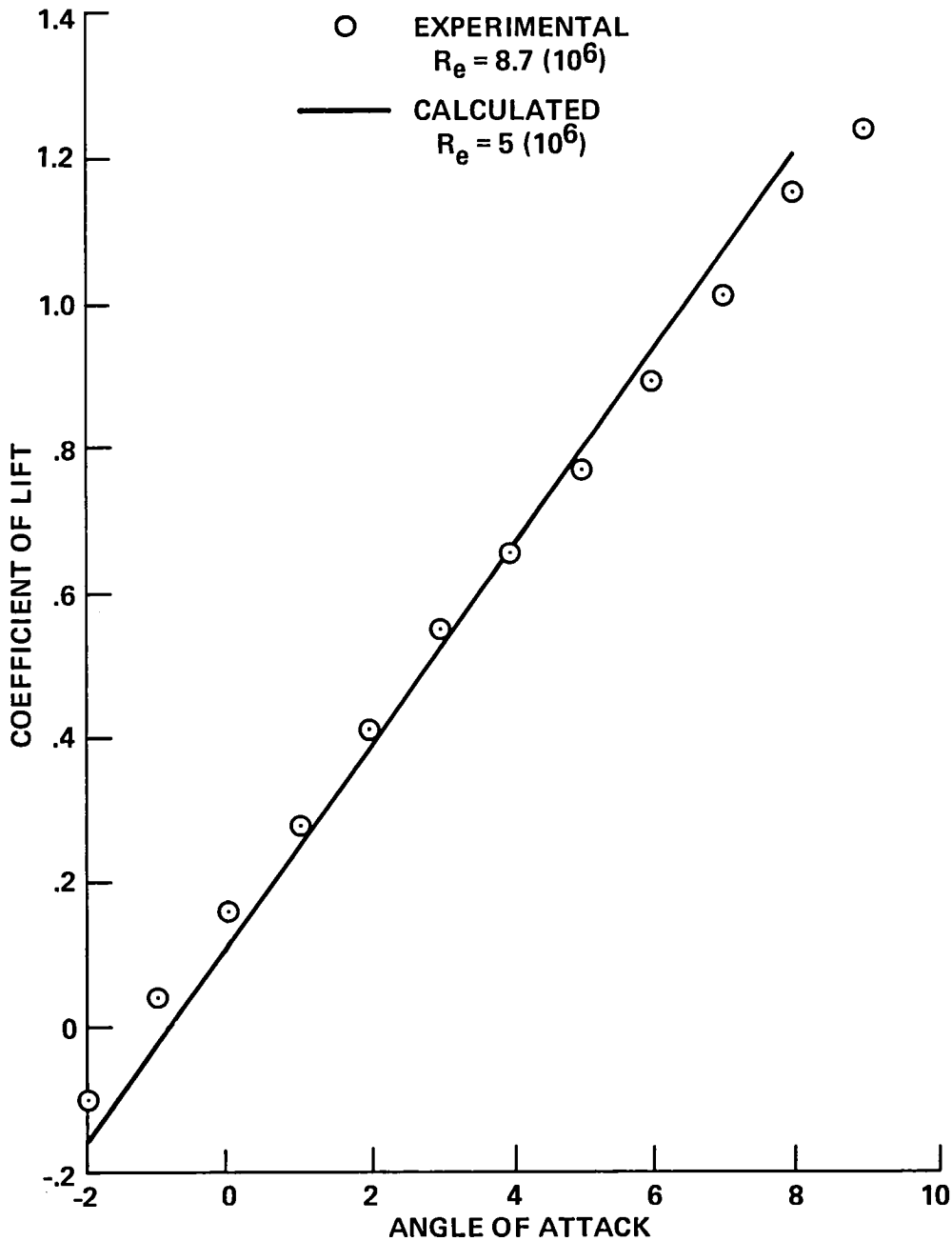

Figure 4.- Boeing VR-7 airfoil: coefficient of lift vs angle of attack at M = 0.5.

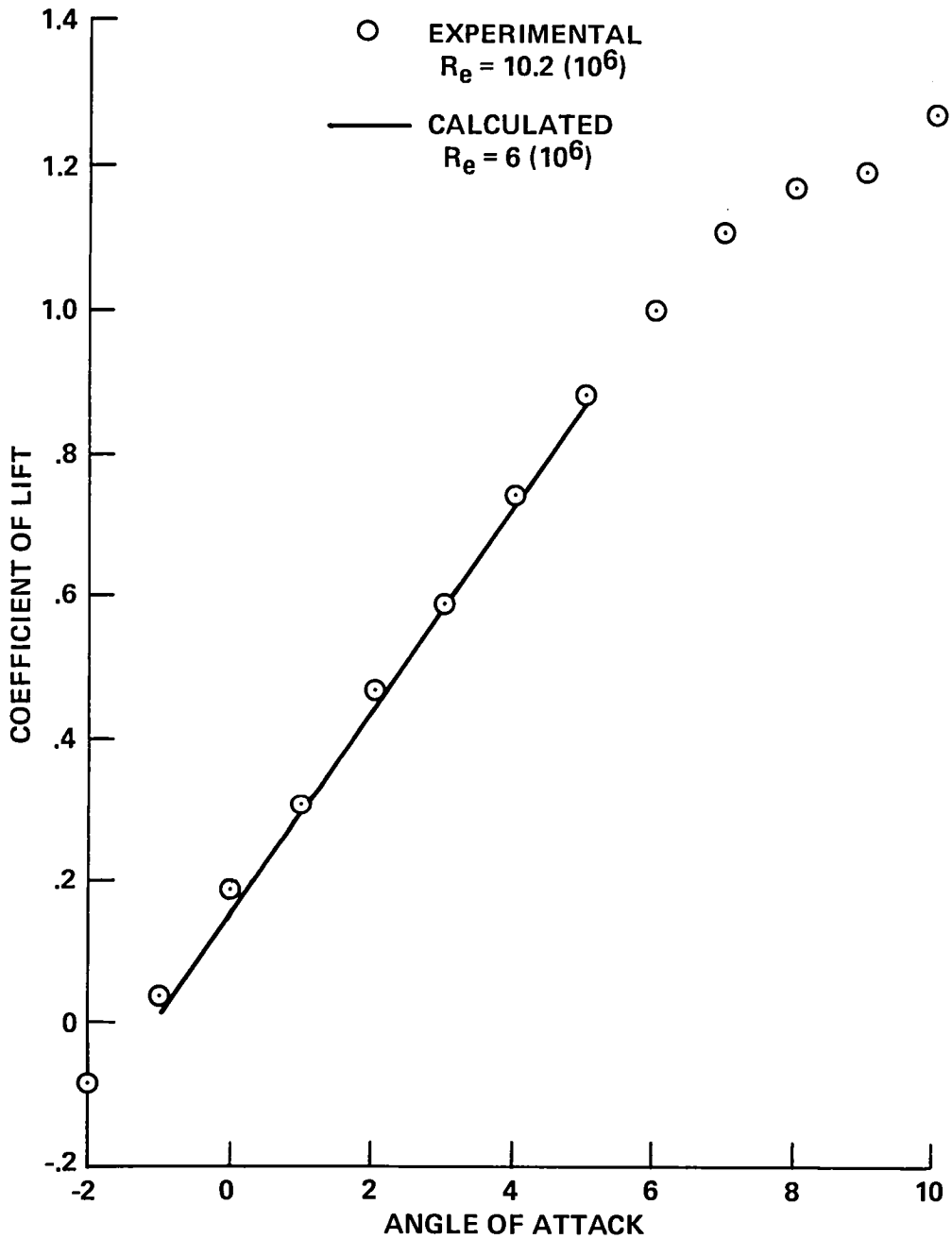

Figure 5.- Boeing VR-7 airfoil: coefficient of lift vs angle of attack at M = 0.6.

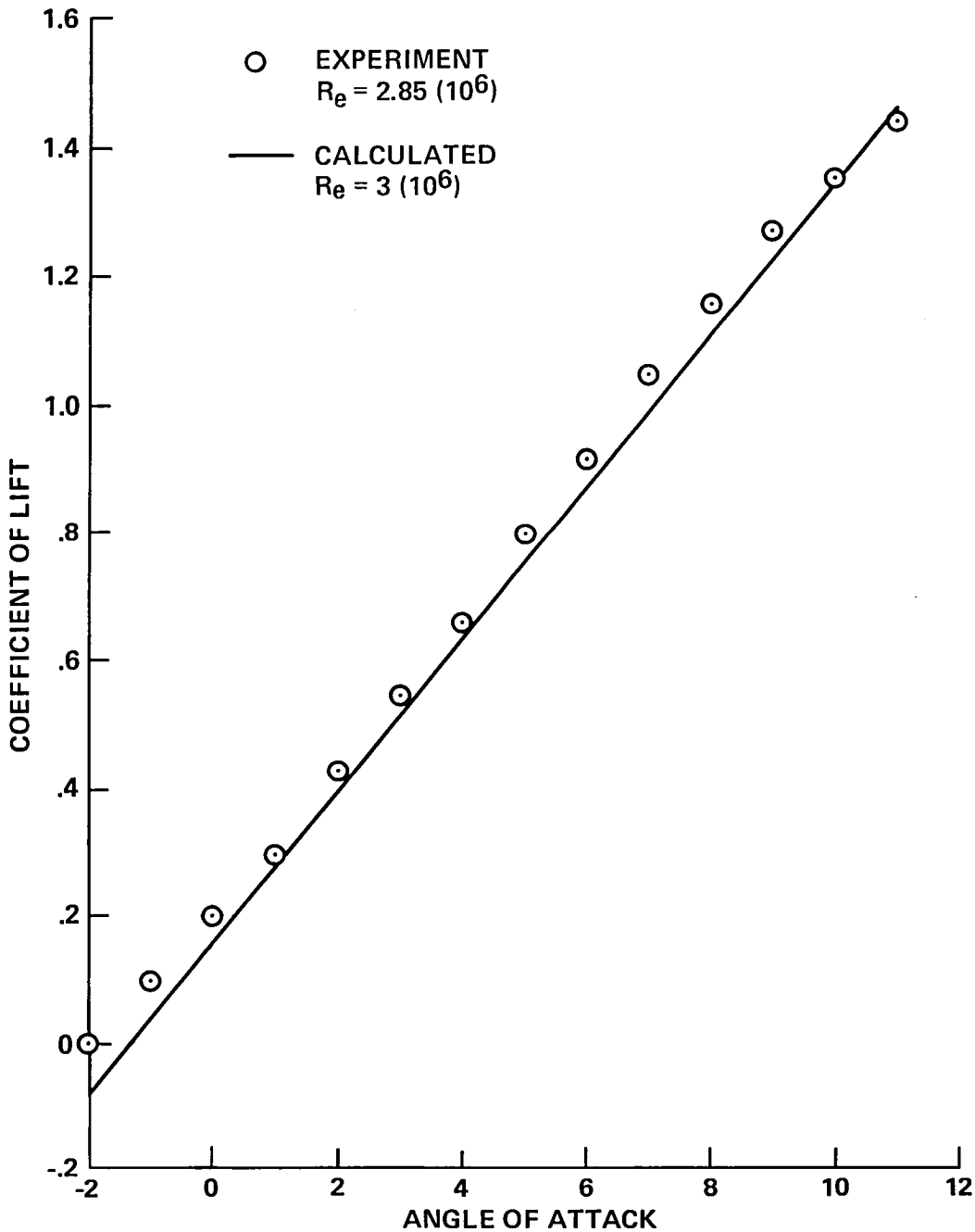

Figure 6.- Wortman 69-H-098 airfoil: coefficient of lift vs angle of attack at M = 0.3.

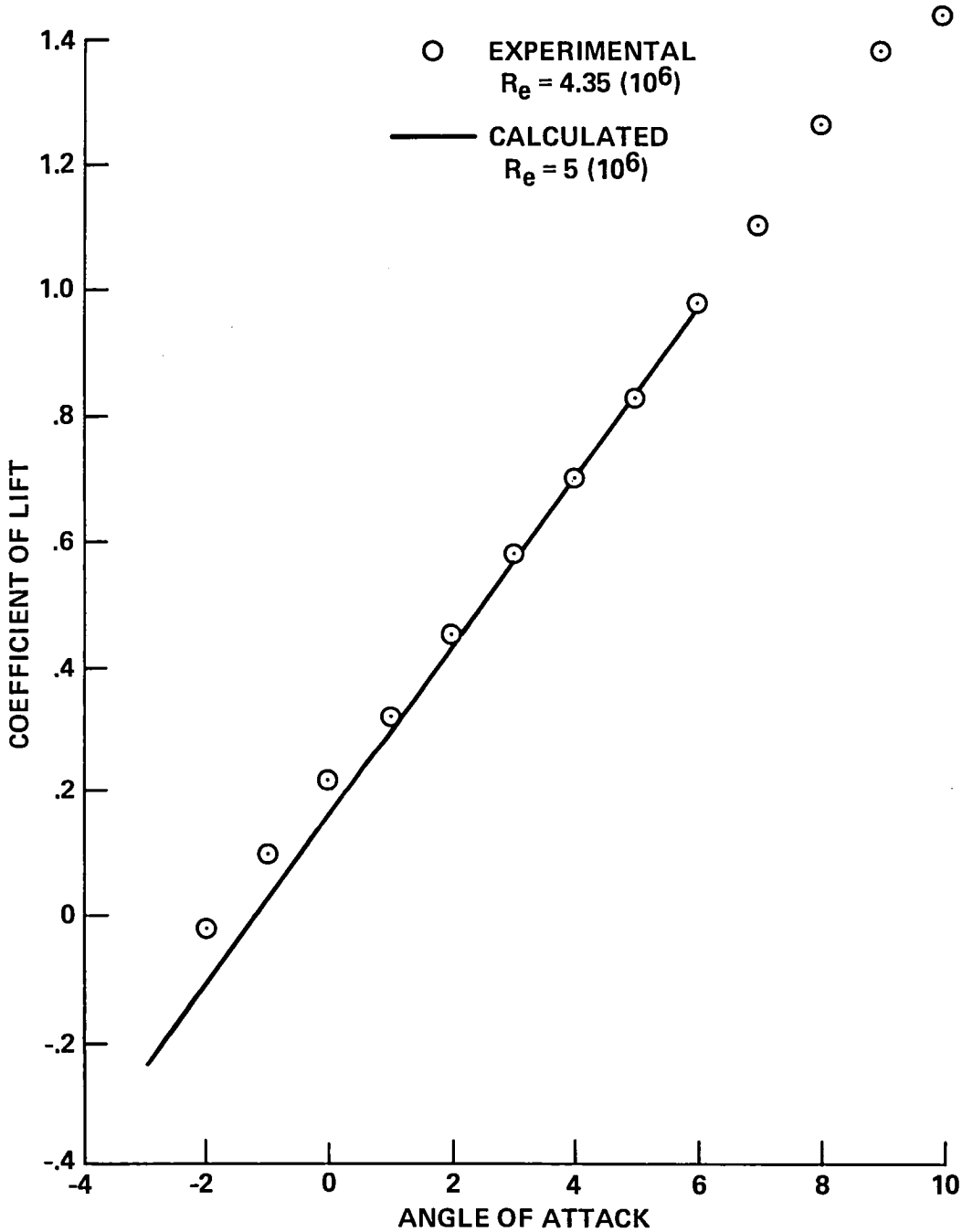

Figure 7.- Wortman 69-H-098 airfoil: coefficient of lift vs angle of attack at M = 0.5.

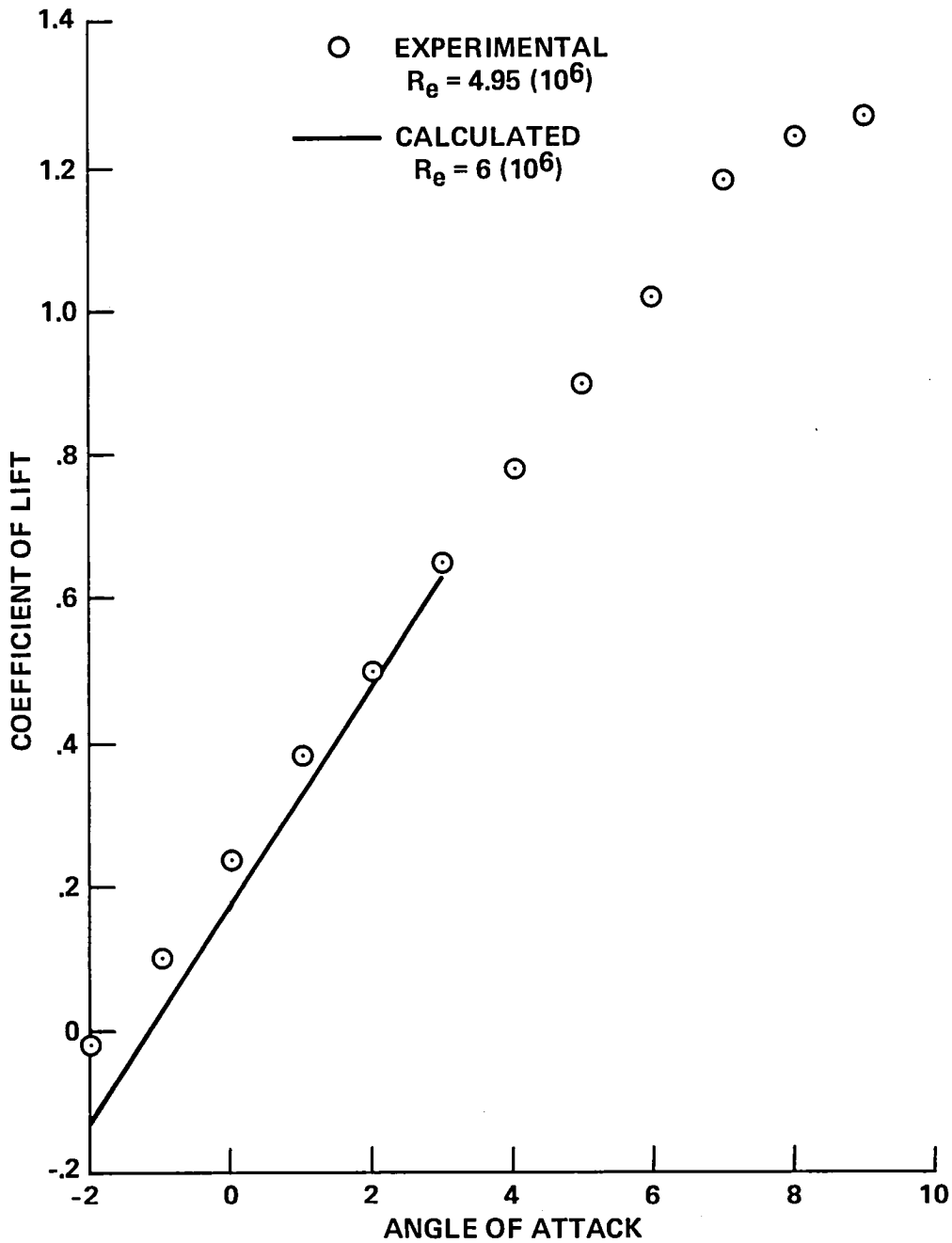

Figure 8.- Wortman 69-H-098 airfoil: coefficient of lift vs angle of attack at M = 0.6.

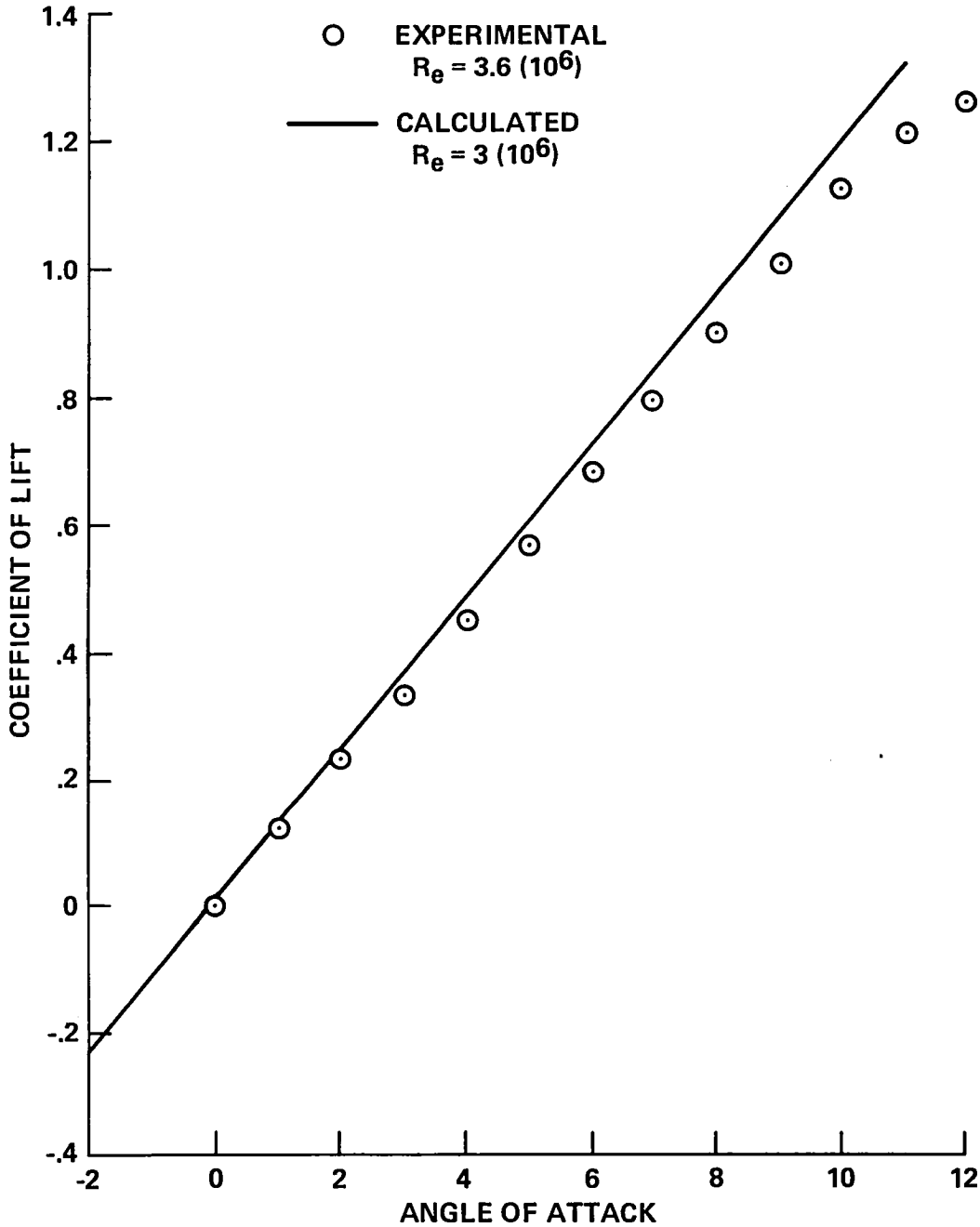

Figure 9.- NACA 0012 airfoil: coefficient of lift vs angle of attack at M = 0.3.

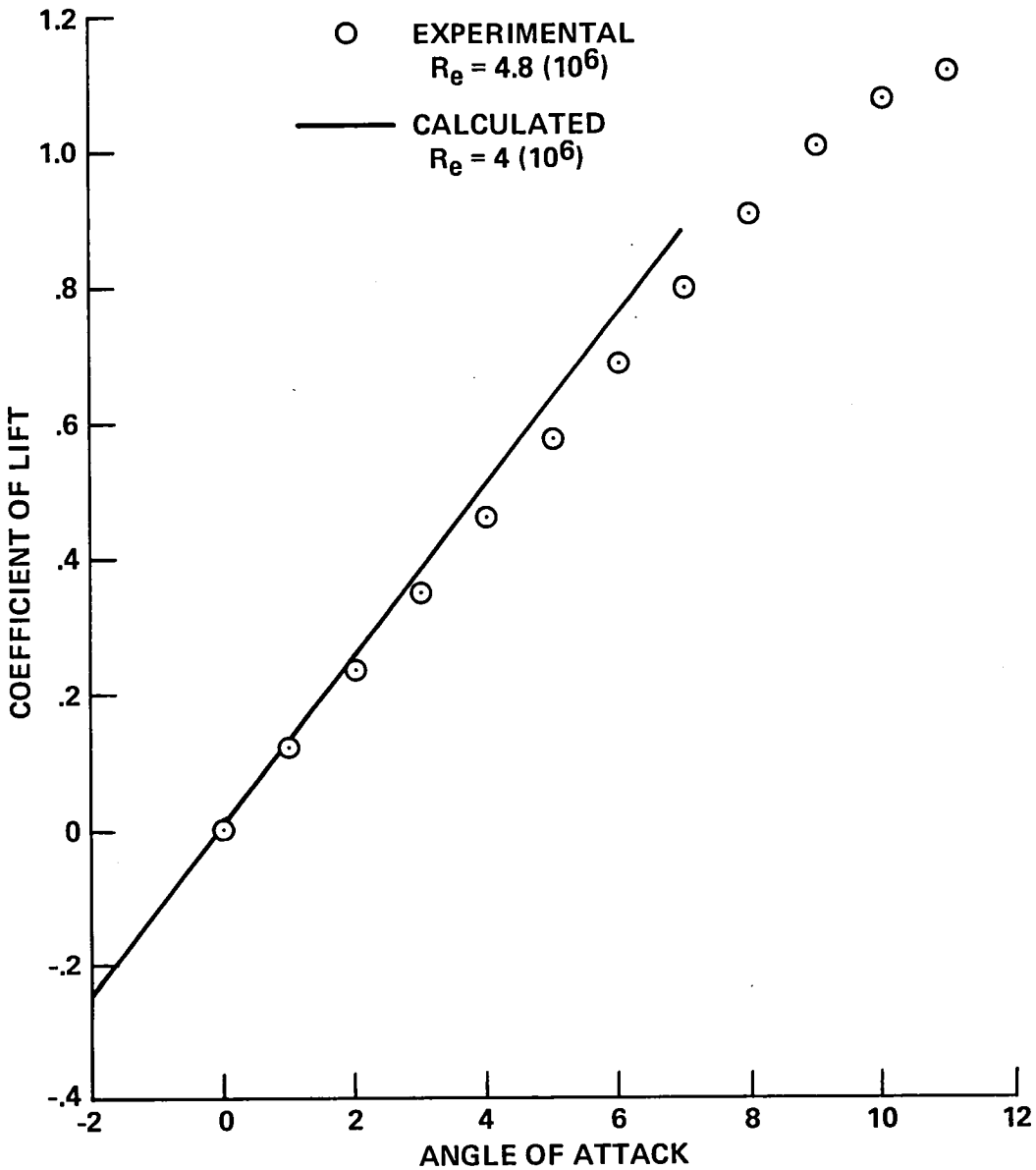

Figure 10.- NACA 0012 airfoil: coefficient of lift vs angle of attack at M = 0.4.

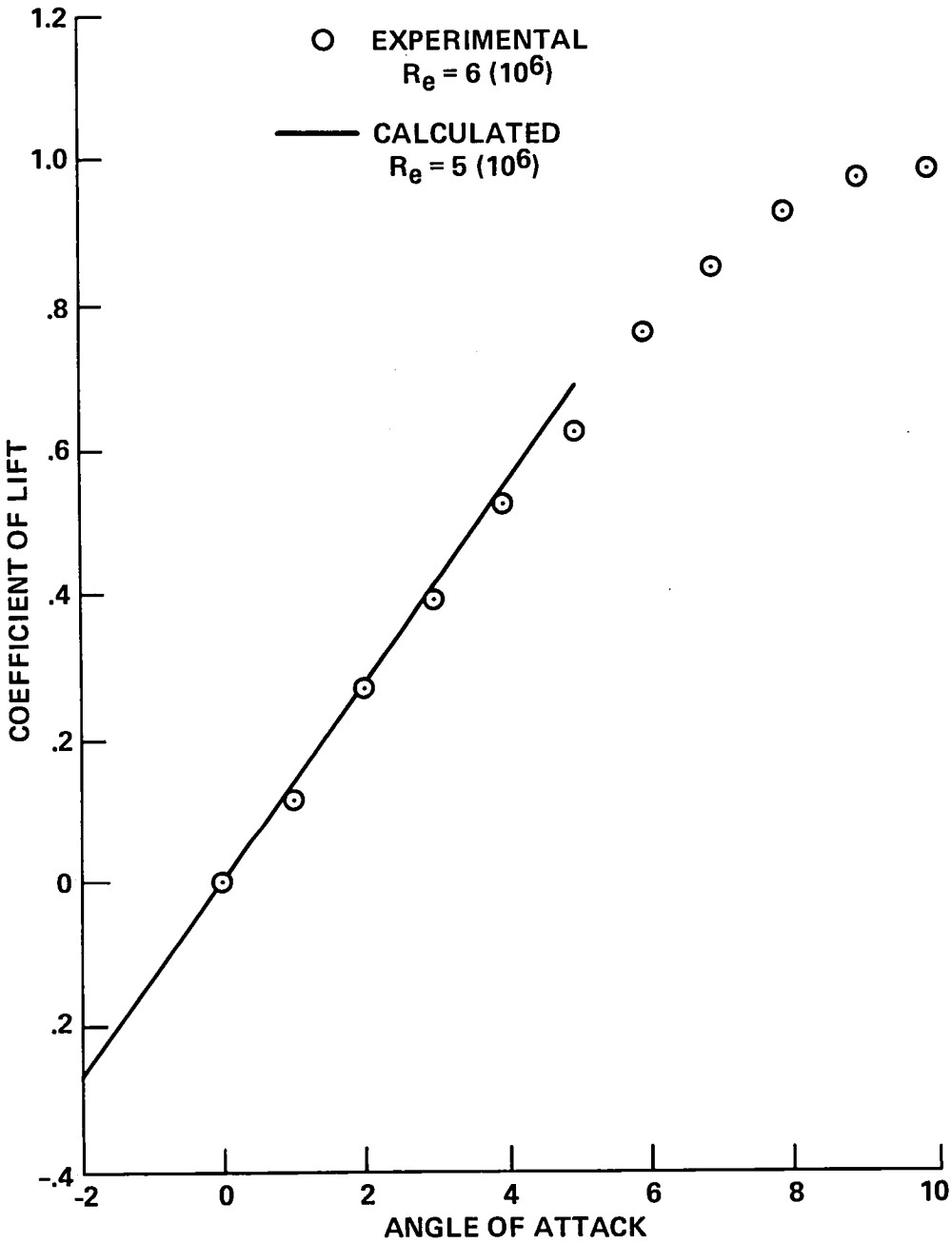

Figure 11.- NACA 0012 airfoil: coefficient of lift vs angle of attack at M = 0.5.

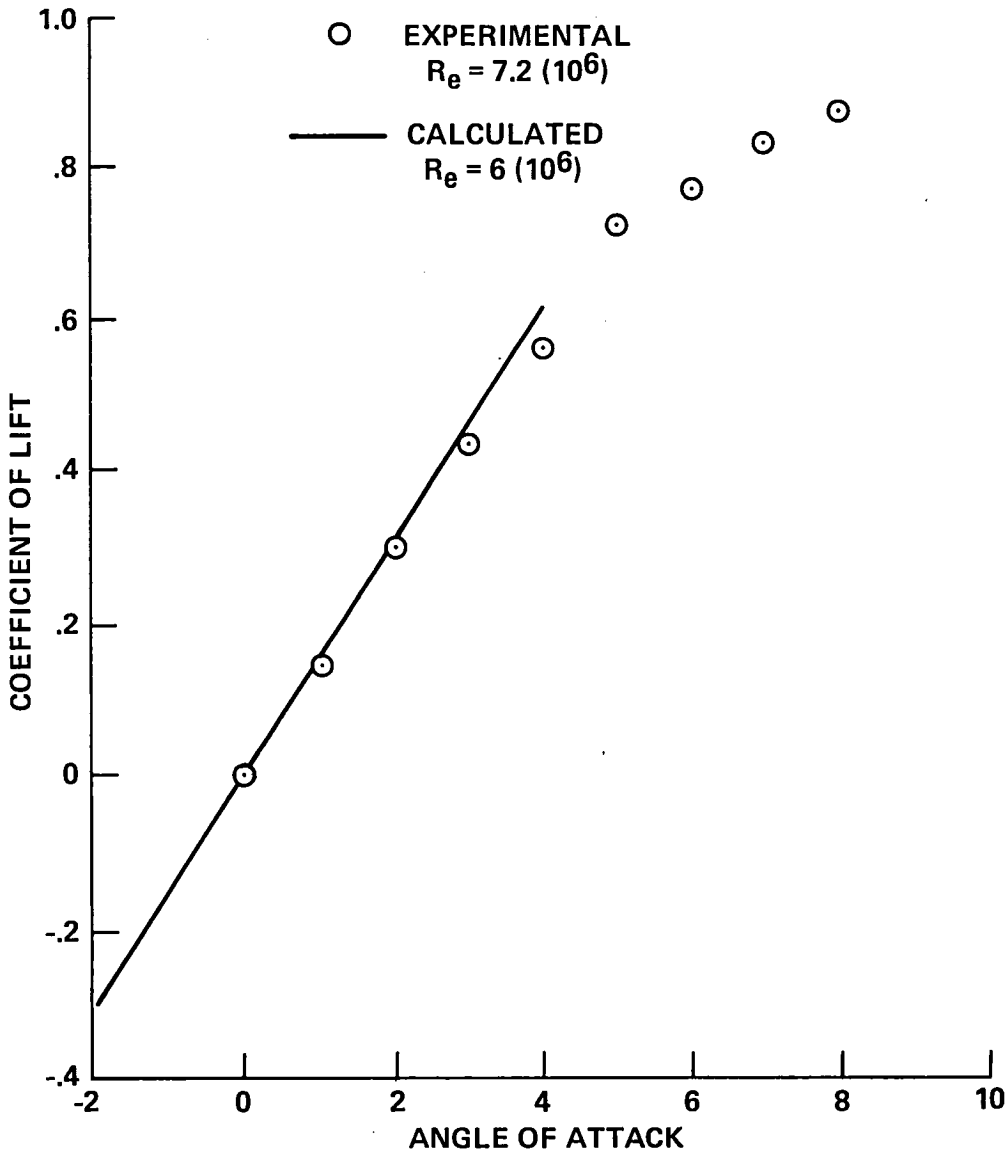

Figure 12.- NACA 0012 airfoil: coefficient of lift vs angle of attack at M = 0.6.

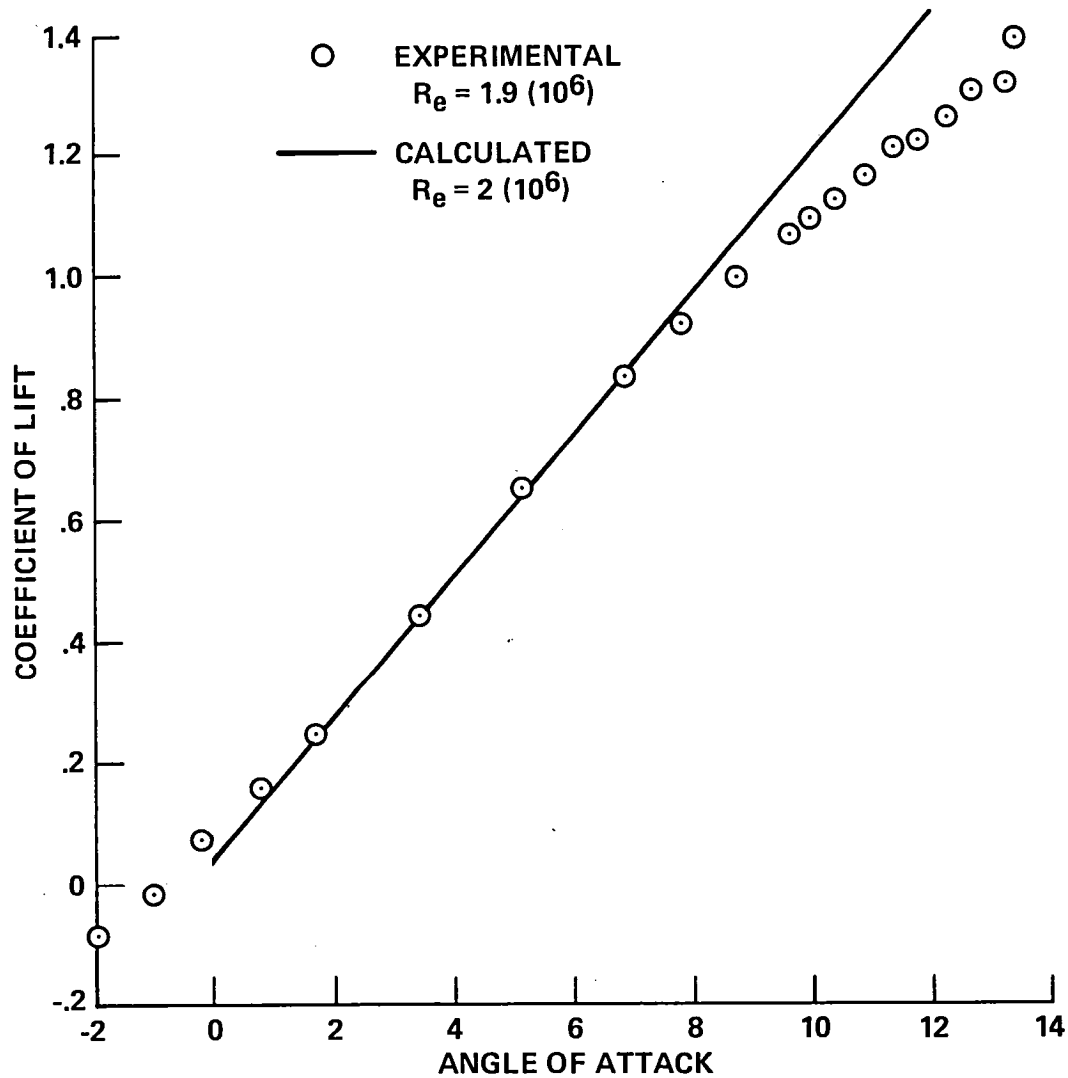

Figure 13.- Ames-1 airfoil: coefficient of lift vs angle of attack at M = 0.2.

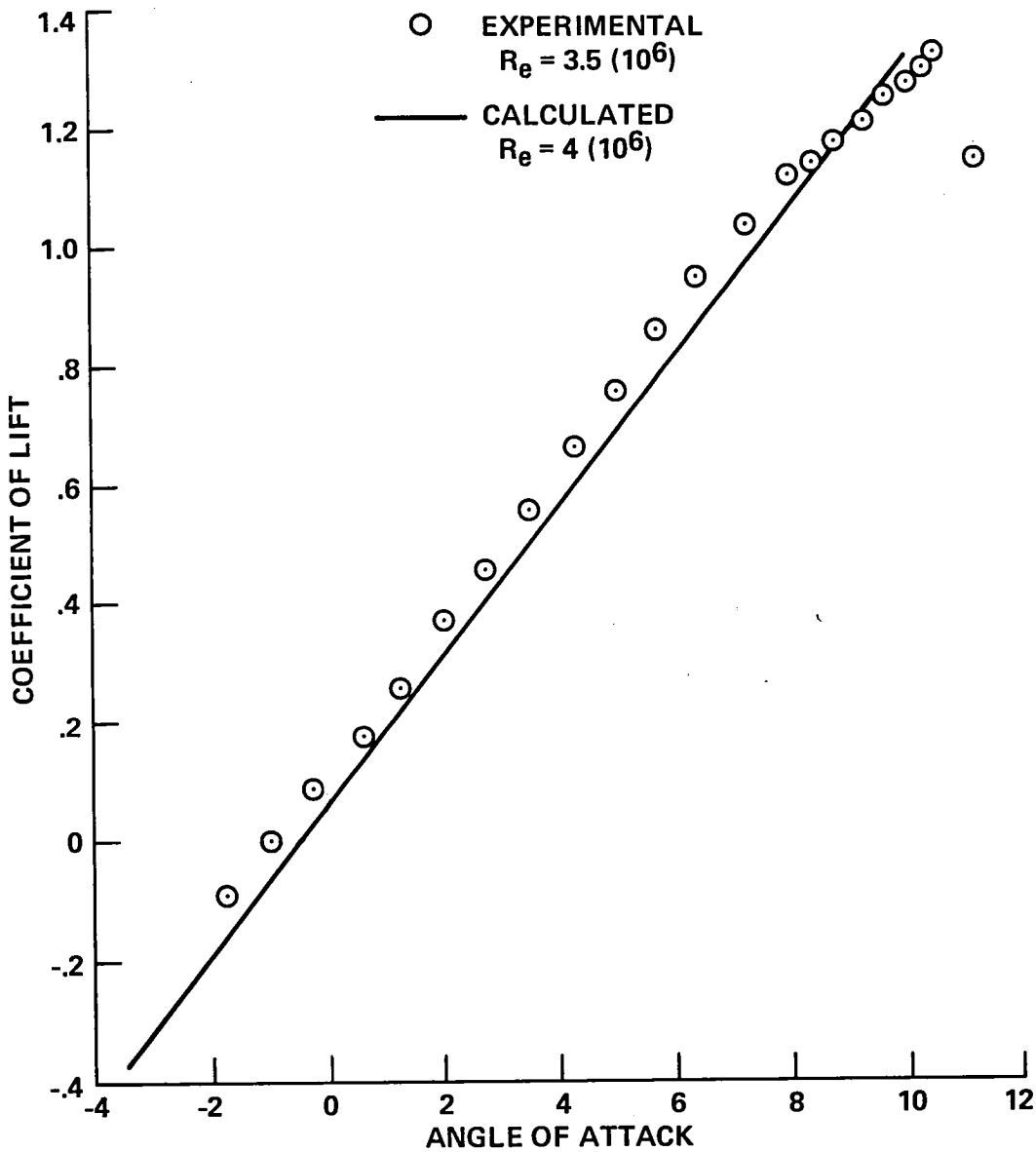

Figure 14.- Ames-1 airfoil: coefficient of lift vs angle of attack at M = 0.4.

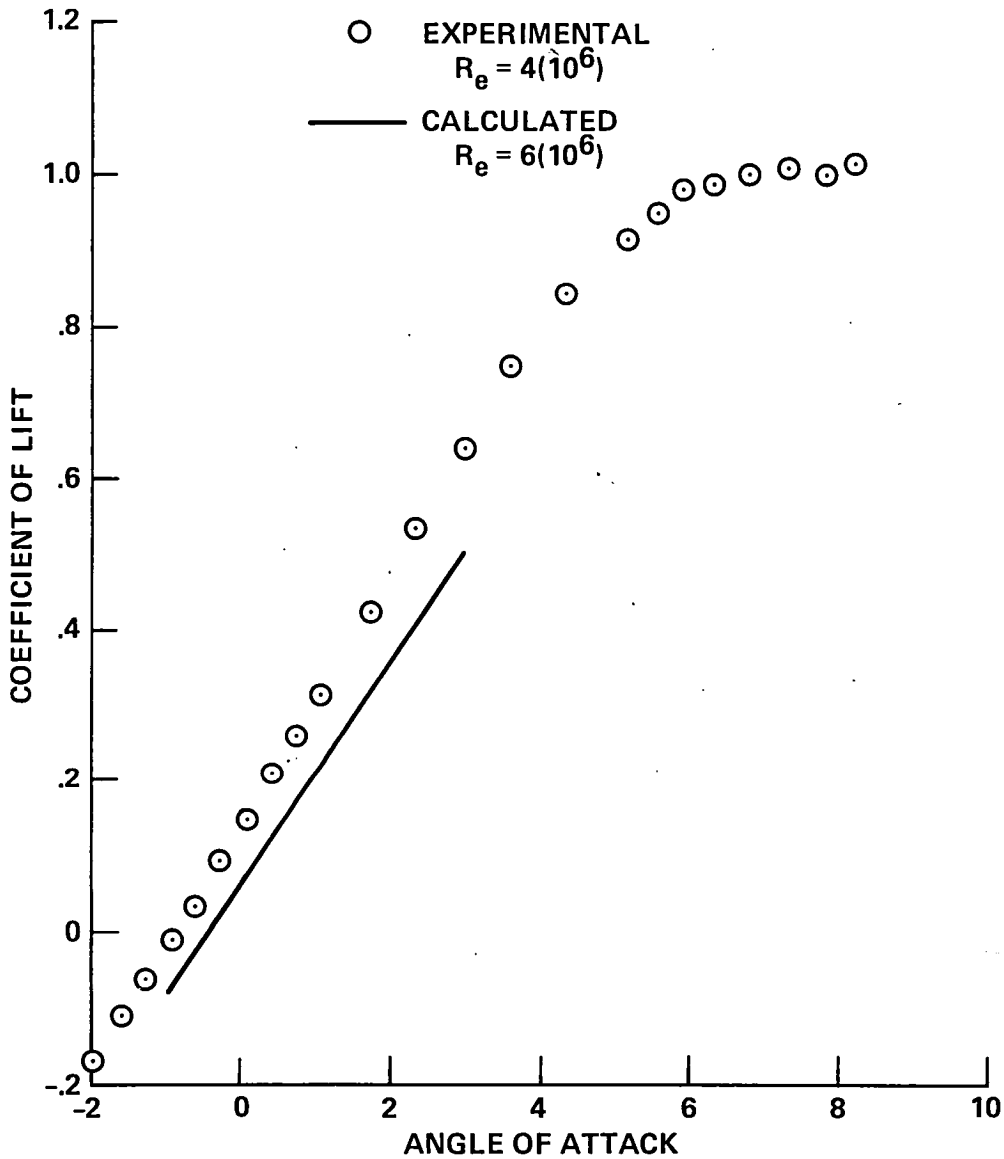

Figure 15.- Ames-1 airfoil: coefficient of lift vs angle of attack at M = 0.6.

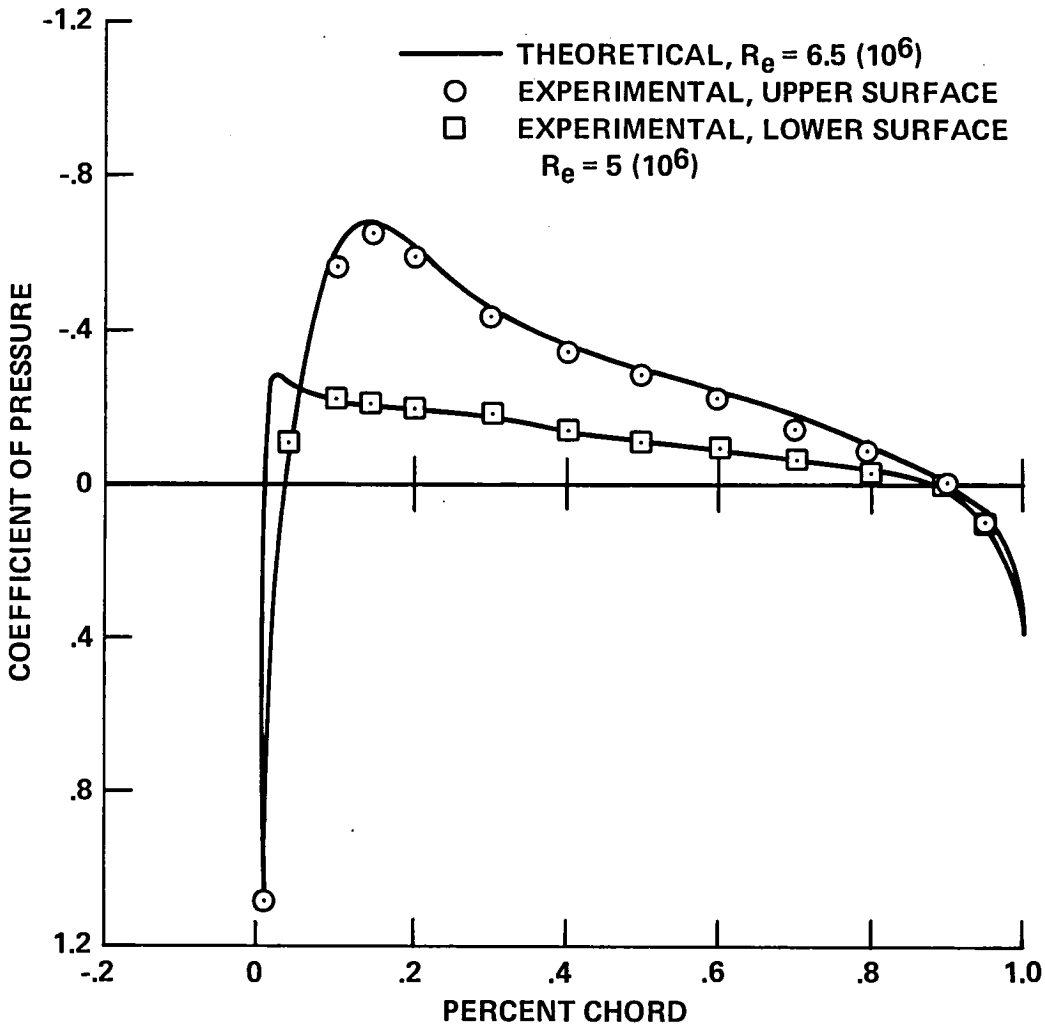

Figure 16.- Wortman 69-H-098 airfoil: coefficient of pressure vs percent cord at M = 0.5, α = 0°.

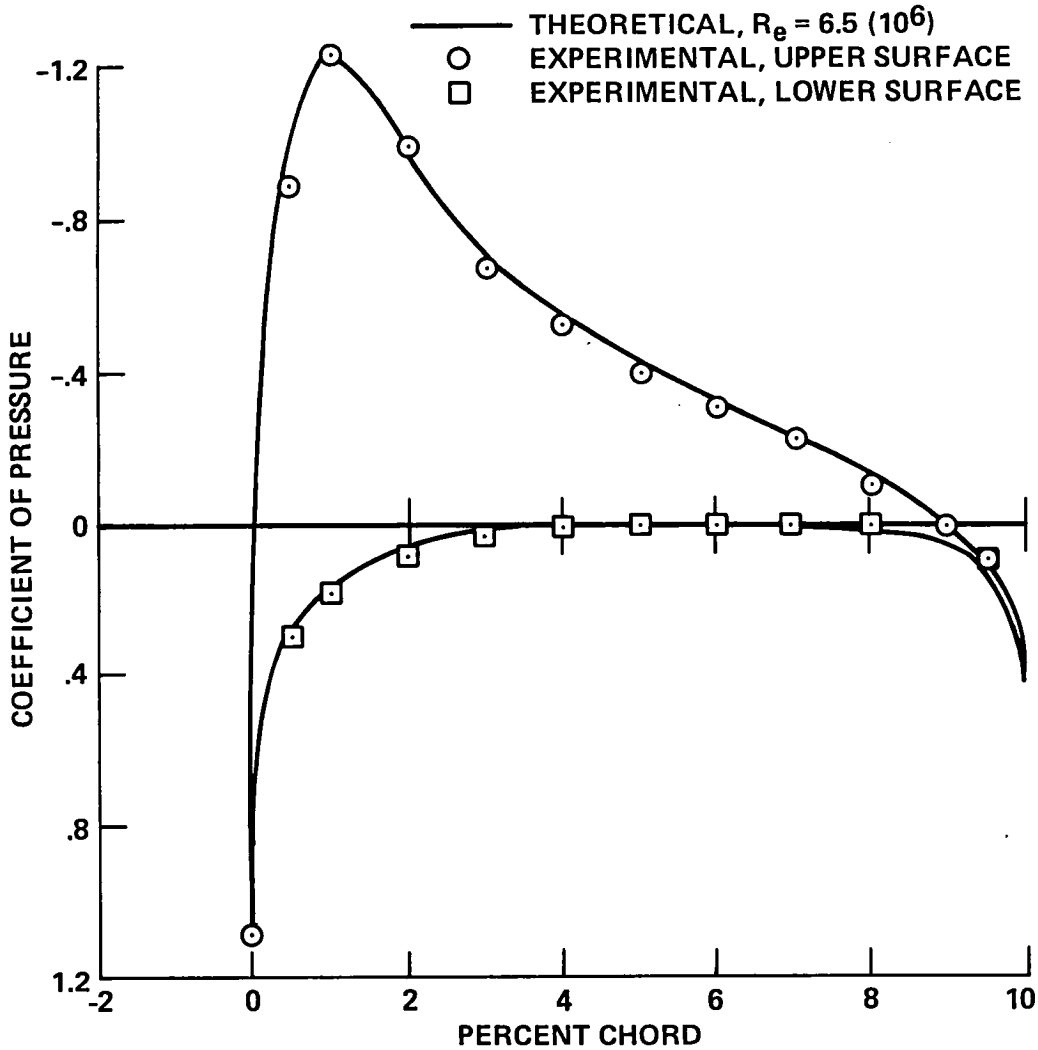

Figure 17.- Wortman 69-H-098 airfoil: coefficient of pressure vs percent cord at M = 0.5, α = 3.0°.

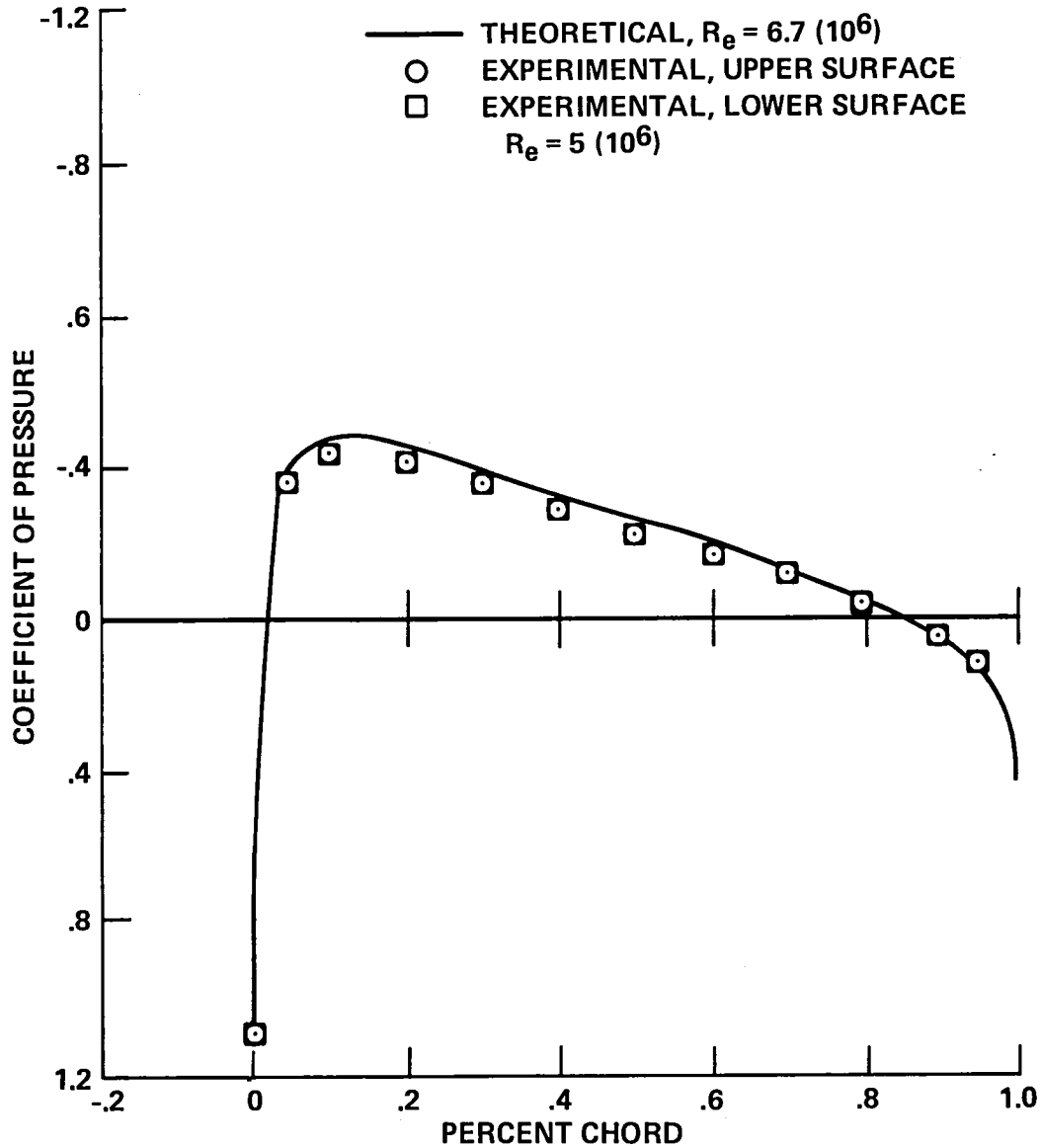

Figure 18.- NACA-0012 airfoil: coefficient of pressure vs percent cord at $M = 0.5$, $\alpha = 0°$.

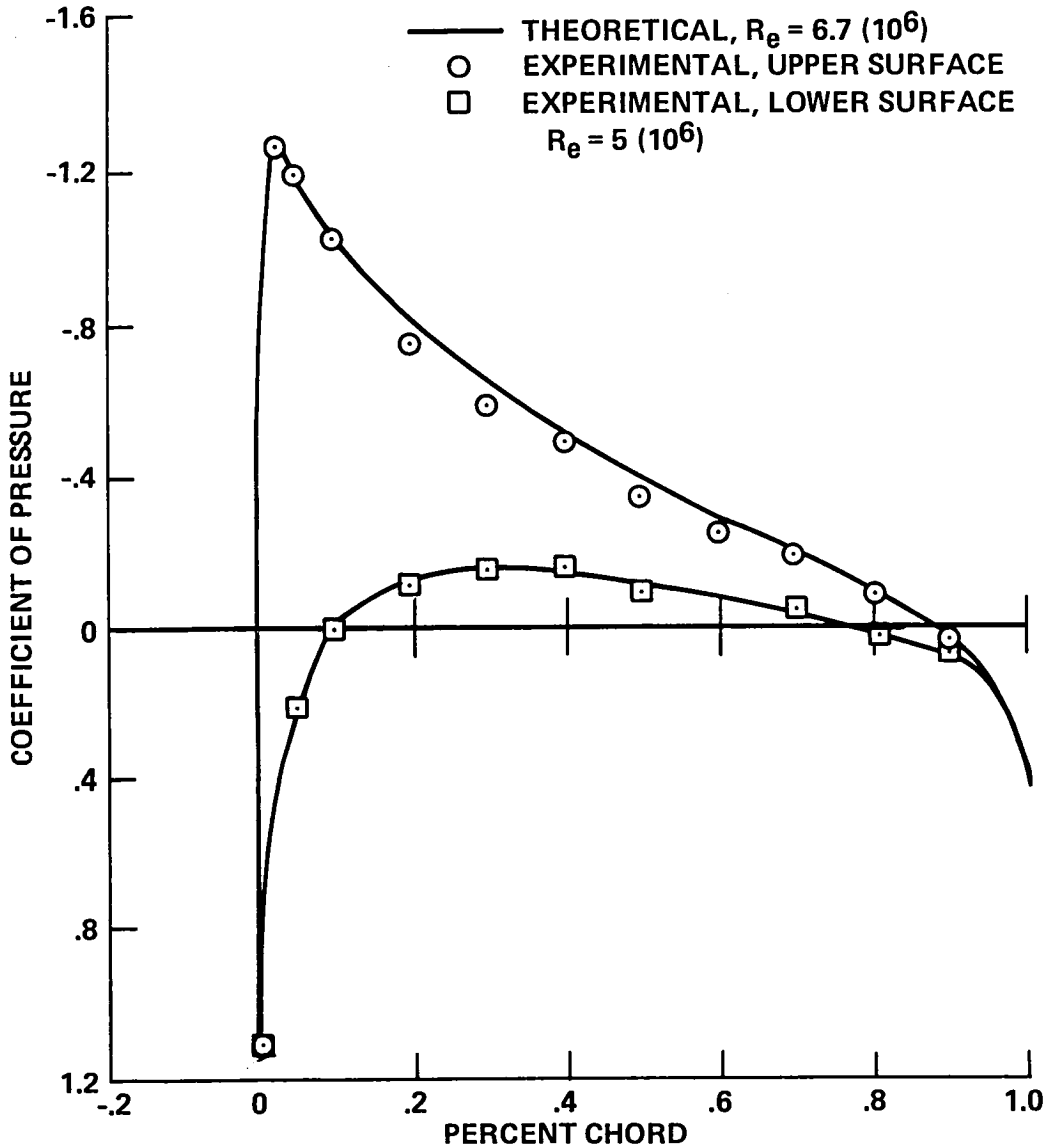

Figure 19.- NACA-0012 airfoil: coefficient of pressure vs percent cord at $M = 0.5$, $\alpha = 3.0°$.

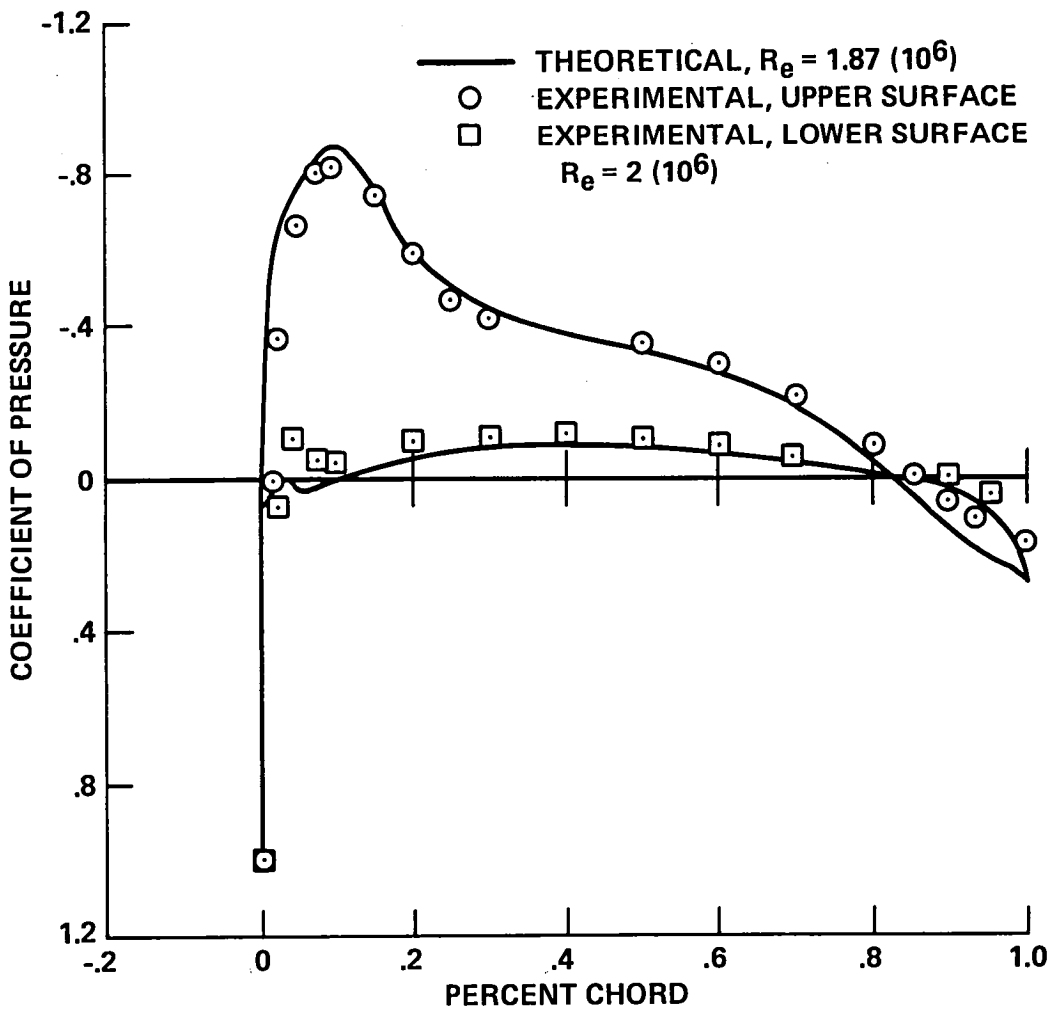

Figure 20.- Ames-1 airfoil: coefficient of pressure vs percent chord at M = 0.20, α = 2°.

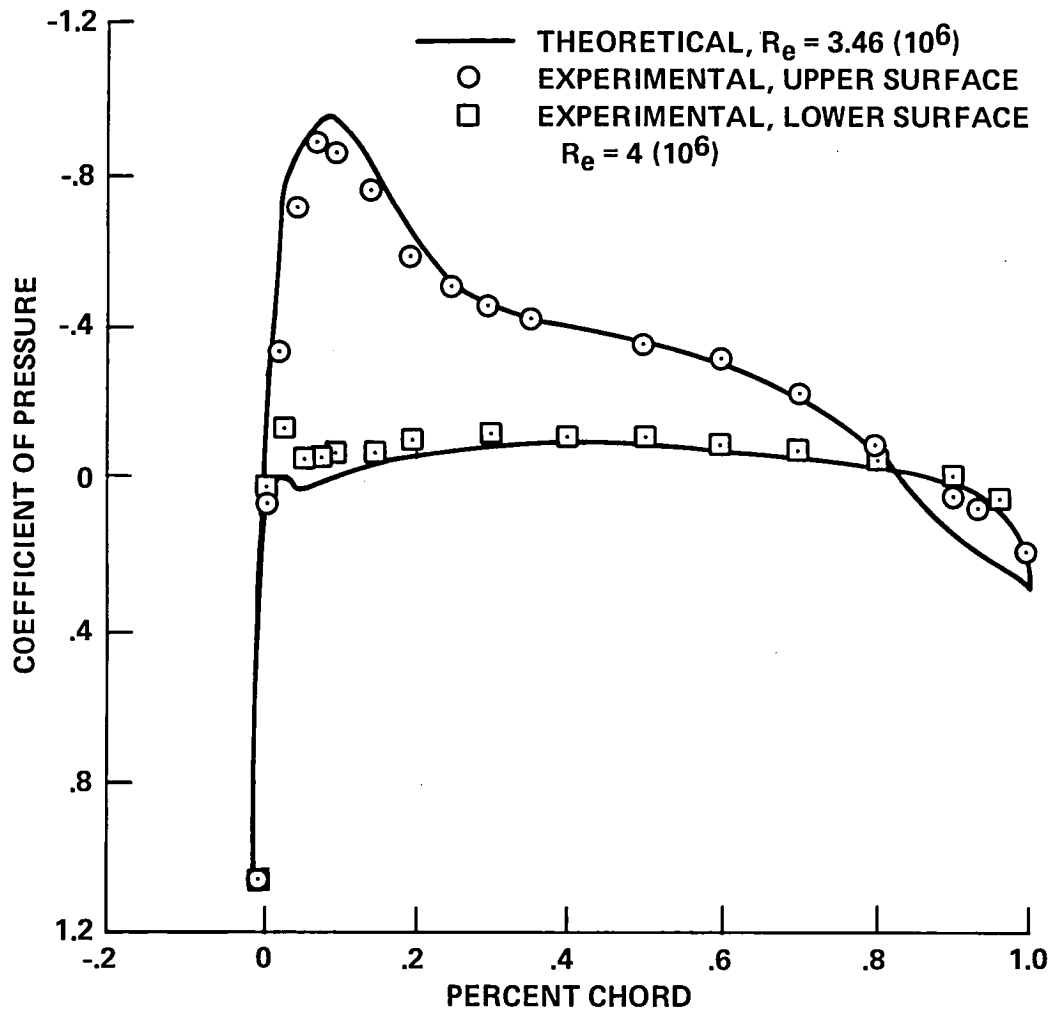

Figure 21.- Ames-1 airfoil: coefficient of pressure vs percent chord at M = 0.4, α = 2°.

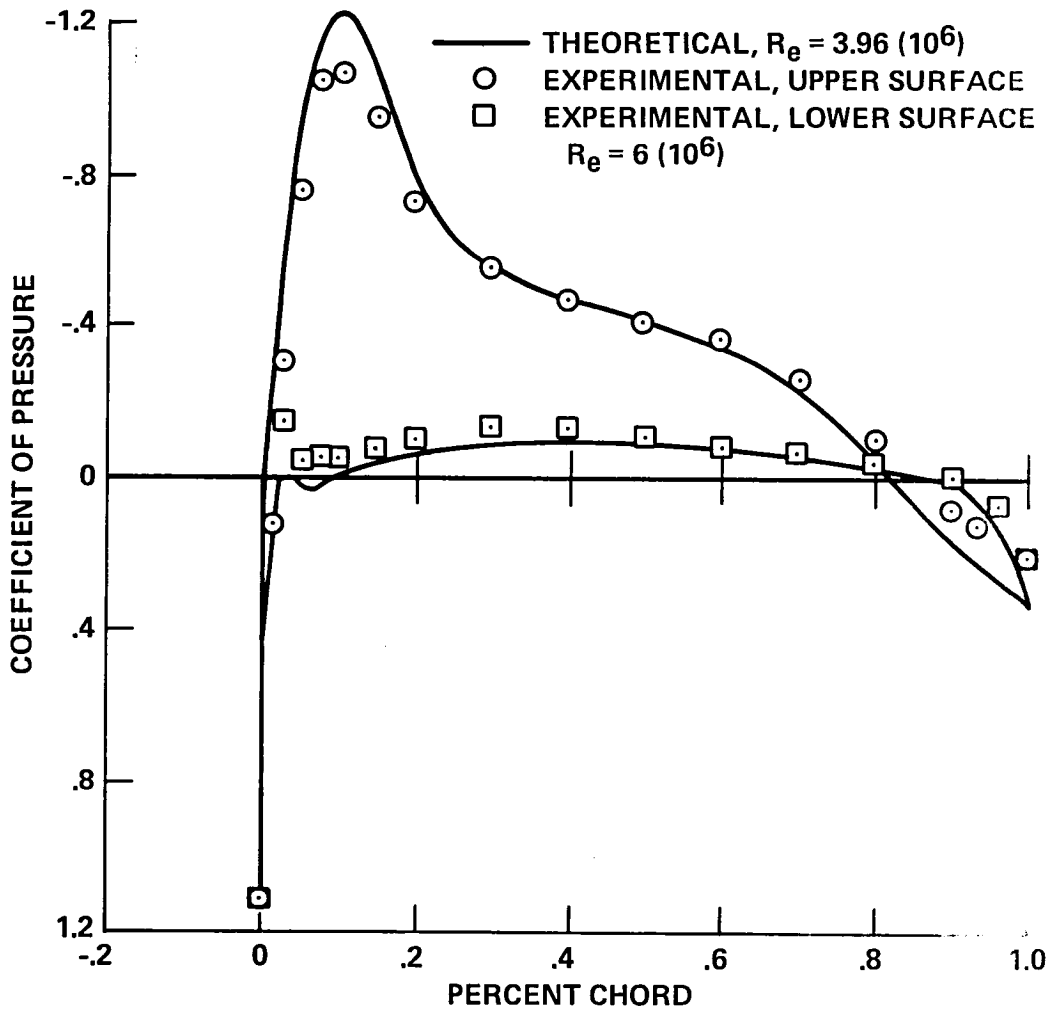

Figure 22.- Ames-1 airfoil: coefficient of pressure vs percent chord at M = 0.6, α = 2°.

1. Report No.	2. Government Accession No.	3. Recipient's Catalog No.
NASA TM-81160		

4. Title and Subtitle	5. Report Date
A COMPARISON OF CALCULATED AND EXPERIMENTAL LIFT AND PRESSURE DISTRIBUTIONS FOR SEVERAL HELICOPTER ROTOR SECTIONS	6. Performing Organization Code
7. Author(s)	8. Performing Organization Report No.
John Conlon	A-8029
9. Performing Organization Name and Address	10. Work Unit No.
Ames Research Center, NASA Moffett Field, Calif. 94035	505-10-21
	11. Contract or Grant No.
12. Sponsoring Agency Name and Address	13. Type of Report and Period Covered
National Aeronautics and Space Administration Washington, D.C. 20546	Technical Memorandum
	14. Sponsoring Agency Code

15. Supplementary Notes

16. Abstract

The use of computational techniques in predicting lift coefficients and pressure distributions of two-dimensional airfoil sections was studied. The computer code FL06/IBL was used to solve the compressible, two-dimensional flow about four different airfoil sections. The lift coefficients of the airfoils were calculated at various angles of attack at subsonic Mach numbers. These calculated lift coefficients were then compared with experimental data. Good agreement between the experimental and calculated data in both lift-curve slope and values of lift coefficient was obtained. For three of the airfoils, calculated pressure distributions were also compared with experimental results for selected cases of Mach numbers and angles of attack; agreement between the calculated and experimental values was excellent.

17. Key Words (Suggested by Author(s))	18. Distribution Statement
Computational aerodynamics Airfoils Aerodynamics	Unlimited STAR Category — 02

19. Security Classif. (of this report)	20. Security Classif. (of this page)	21. No. of Pages	22. Price*
Unclassified	Unclassified	33	$4.50

*For sale by the National Technical Information Service, Springfield, Virginia 22161